INFLUENCE OF REACTIVE ION ETCHING ON THE MINORITY CARRIER LIFETIME IN P-TYPE SI

P.N.K. Deenapanray[1], C.S. Athukorala[1], D. Macdonald[2], V.E. Everett[1], K.J. Weber[1] and A.W. Blakers[1]
[1]Centre for Sustainable Energy Systems, FEIT, The Australian National University, Canberra ACT 0200
email: prakash.deenapanray@anu.edu.au
[2]Department of Engineering, FEIT, The Australian National University, Canberra ACT 0200, email: Daniel.macdonald@anu.edu.au

ABSTRACT: Quasi-steady-state photoconductance (QSSPC) and deep level transient spectroscopy (DLTS) were used to characterize the recombination properties of reactive ion etched p-type Si. The effective lifetime of the plasma-processed samples degraded after etching, with the densities of recombination centers increasing linearly with etch time, before reaching a plateau. Evidence is provided for the long-range (> 2 µm) migration of defects in the samples plasma-etched at room temperature. The relationship between rf power and lifetime degradation is also discussed. A defect with energy position at (0.31 ± 0.02) eV was detected by DLTS in RIE p-Si, whereas no defect level was measured in n-type Si. We demonstrate that this energy level could be used to adequately model the injection-dependence of the measured carrier lifetimes using the Shockley-Read-Hall model.
Keywords: Reactive ion etching, Defect, Lifetime, DLTS

1 INTRODUCTION

Plasma (or dry) etching has become a dominant technique in semiconductor processing because it provides highly anisotropic etch profiles with good selectivity. Etching of vias and trenches in SiO_2 is now a critical step in the fabrication of multilevel interconnects for the ultra-large scale integration of Si devices, while nanometer-size patterns are routinely transferred onto polysilicon, SiO_2 or Si_3N_4 using plasma etching for fabricating devices and structures as diverse as semiconductor memories, photonic crystals, high electron mobility transistors, laser diodes, and microelectromechanical systems [1]. In contrast, plasma etching has not made a significant impact in the field of photovoltaics (PV), where the fabrication of silicon solar cells is still heavily reliant on wet chemistry. One significant barrier for using dry etching is the creation of damage in the exposed semiconductor that results in the degradation of device performance. There have been few experimental investigations of the influence of plasma etching on the minority carrier lifetimes in Si [1-3].

Reactive ion etching (RIE) is potentially a key technology in the fabrication of solar cells, such as the micromachined thin-film c-Si cells developed recently at the ANU [4]. For this reason, we have characterized the effect of RIE on the lifetime of minority carriers in both n- and p-type FZ Si. We will demonstrate that DLTS and QSSPC is a powerful combination to characterize the electrical properties of defects that are relevant to the performance of solar cells.

2 EXPERIMETAL PROCEDURE

RIE was performed in an Oxford PlasmaLab80 system using CHF_3/O_2 plasma. The process pressure was 55 mT and gas flow rates were 50 sccm and 5 sccm for CHF_3 and O_2, respectively. Samples were placed on the water-cooled electrode (23°C) that was powered by a 13.56 MHz rf generator. In this study, only the exposure time or rf power was varied. We used both B- or P-doped FZ wafers. The p-type samples had resistivities of 0.75-1.25 O cm and 140-150 O cm, while the n-type FZ wafers had resistivities of 0.8-1.5 O cm and >100 O cm. In one experiment, 150 O cm p-FZ samples were exposed to RIE for 15 s to 25 min using either 50 W or 200 W rf power. We typically use 200 W etching of dielectrics in the fabrication of our novel thin-film Si solar cells [4]. In a second experiment, 150 O cm p-FZ and 100 O cm n-FZ samples were exposed simultaneously to the plasma for 30 s but at different rf powers. Additionally, 1 O cm p-FZ and 100 O cm n-FZ samples were exposed at 200 W for either 30 s or 5 min. After RIE, the samples were chemically cleaned prior to light phosphorous diffusion and oxidation. Surface passivation of samples was completed with a forming gas anneal at 400°C. The use of control samples allowed the recombination rate due to all processes other than those caused by RIE, such as recombination at the surfaces, and recombination in the bulk due to Auger recombination and potential contamination arising from the annealing, etching and cleaning steps, to be measured.

The carrier lifetimes, t_{eff}, were determined using the quasi-steady-state photoconductance method (QSSPC) [5], which measures the lifetime as a function of excess carrier density $\boldsymbol{D}n$. Deep level transient spectroscopy (DLTS) was performed on the control and plasma-etched 1 O cm p-FZ and 1 O cm n-FZ samples using a modified lock-in-type setup.

3 IMPACT OF RIE ON LIFETIME

Figure 1 shows the effect of both RIE depth etched (i.e. time) and rf power on lifetime in high-resistivity p-Si. We have plotted $1/t_{eff}$ which is proportional to the concentration of defects in the sample [1].

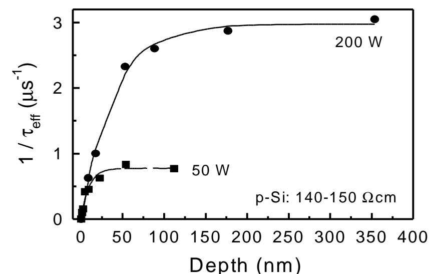

Figure 1: Effect of RIE on effective lifetime.

In Fig. 1, t_{eff} was measured at $?n = 1 \times 10^{14}$ cm^{-3}. Two regimes can be identified in Fig. 1, namely an initial build up of defects followed by an equilibrium level. The latter arises when the creation of damage by ion bombardment is counter balanced by damage removal by the combination of physical and chemical etching. The plateau is reached earlier at the lower rf power, which is related to the correspondingly lower dc self-bias generated on the electrode that holds the sample. This reveals that the etch rate decreases slower than the extent of damage by ion bombardment when the rf power is decreased. Figure 1 reveals that damage creation proceeds at a faster rate than etching of the damaged layer in the initial stage of RIE. It is worth pointing out that in our RIE system, the production of damage due to the self-bias generated on the electrode holding the sample cannot be decoupled from the overall etch process.

3.1 Effect of post-RIE Si etching

In order to establish the depth of the sample that becomes defective after RIE, we have performed post-RIE Si-etching of samples, prior to their high temperature surface passivation and characterization. Figure 2 shows the results for the high-resistivity p-Si etched at 200 W for either 1 min or 5 min. There are two points to note: (1) lifetime is recovered only partially even after removing ~2 µm of the exposed surfaces, and (2) it would appear that the recovery of the lifetime decreases monotonically with increasing amount of Si etched. These observations reveal the long-range migration of defects created by RIE at 23°C in the samples. Prolonged post-RIE Si etching is required to establish whether full recovery of the initial lifetime of the order of 1 ms can be achieved.

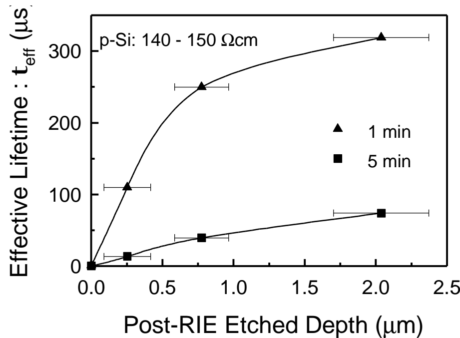

Figure 2: Effect of post-RIE Si etching on lifetime

3.2 Effect of rf power

The variation of carrier lifetime was measured for the 150 O cm p-FZ and the 100 O cm n-FZ samples as a function of rf power as shown in Fig. 3 for $?n = 1 \times 10^{14}$ cm^{-3}. Samples were etched simultaneously for 30 s, which corresponds to the maximum over-etch time for dielectric layers deposited on our Si substrates as part of the novel solar cell fabrication process mentioned earlier. Consequently, the carrier lifetimes do not reflect the steady-state concentrations of defects at the different rf powers. Figure 3 shows that the minority carrier lifetimes in reactive ion etched n- or p-type Si are similar.

Given the large difference between the resistivity of the n- and p-type samples used here, we have determined the doping

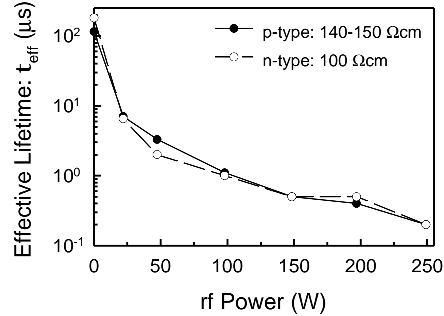

Figure 3: Effect of rf power on effective lifetime

concentration of the high-resistivity n- and p-type samples using dark conductance measurements. The doping concentrations have been measured to be approximately 6×10^{13} cm^{-3} and 3.5×10^{13} cm^{-3} for the p- and n-type wafers, respectively. It is approximately true then that N_A ~ N_D for these high-resistivity wafers. This observation is important since it reveals that, should a single deep level defect be responsible for the lifetime changes, the minority and majority carrier capture cross-sections of the defect should also be similar when $p_0 = n_0$ or $N_A = N_D$ [7].

4 DLTS MEASUREMENTS

One limitation of single-temperature QSSPC measurements is that it is difficult to extract any direct information regarding the "signatures", such as energy position, E_t, in the band gap and capture cross section, s, of the recombination centres. One technique that can provide such information about defects is DLTS.

Since we have used Schottky diodes for DLTS measurements, the spectra obtained from n- and p-Si do not provide any information regarding deep levels in the lower- and upper-half of the band gap, respectively. Nevertheless, the combination of DLTS measurements in n- and p-type Si, together with the rf power dependence of lifetime, provide us with significant information regarding the properties of defects that may be responsible for lifetime degradation in reactive ion etched samples.

Figure 4 shows that RIE did not introduce any defects in the upper half of the band gap of n-Si (solid triangles). On the other hand, the spectrum taken from an etched p-Si sample reveals the presence of two discrete defects. These hole traps are labeled A(0.54 eV) and B(0.32 eV). However, the DLTS spectrum taken from the control p-Si already reveals the presence of A(0.54 eV), clearly indicating that RIE introduced B(0.32 eV). The energy position in the band gap and capture cross section of B(0.32 eV) and B(0.54 eV) are $E_t = E_V + (0.32 \pm 0.02)$ eV and s_a ~ 4.2×10^{-14} cm^2, and $E_t = E_V + (0.54 \pm 0.02)$ eV, and s_a ~ 8.5×10^{-14} cm^2, respectively (are these cross sections for electrons or

holes?). The "signatures" of the defects were determined from Arrhenius plots of $\ln(T^2/e_h)$ vs $1000/T$, where eh is the emission rate [1].

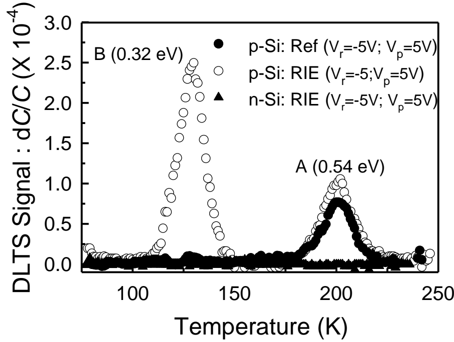

Figure 4: DLTS spectra taken from low-resistivity p- (circles) and n-Si (solid triangle).

Although DLTS does not provide any direct information regarding the structure of defects, one can still make an informed estimate of the structure of a defect by comparing its signature to the signatures of defects reported previously in the literature and by comparing the annealing properties of the defect with those of known defects. In a previous study, we used this methodology to conclude that A(0.54 eV) was probably the B_i-B_s-H complex [1]. Bias-dependent DLTS measurements had shown that A(0.54 eV) was confined within the top 0.6 μm of the plasma-etched sample. The H-related structure was consistent with the in-diffusion of hydrogen during chemical etching in HF solution. Further, A(0.54 eV) displayed a low thermal stability (100-150°C) similar to that of the H-related complex.

In our earlier study, we had suggested that B(0.32 eV) was probably a B_i-related defect [1]. However, the results shown in Fig. 3 indicate that the defect responsible for the recombination was introduced equally in n- and p-type Si by RIE. This then excludes any defect related to dopant atoms. Likely candidates that can account for the structure of B(0.32 eV) in both n- and p-type Si are C and O impurities. In a study of electron-irradiation-induced defects in B- or Ga-doped Cz Si [7], we have reported the energy position of the C_i-O_i complex to be at 0.33 eV above the valence band in B-doped Cz Si. The C_i-O_i complex is known to be an efficient recombination centre [8]. However, the thermal stability of B(0.32 eV) in the temperature range 200-250°C we have measured [1] is relatively low compared to that reported in the literature for the C_i-O_i complex [9]. Further characterization of this defect is required before a more definitive conclusion can be made regarding its structure.

5 SRH MODELLING

We have used the "signature" of B(0.32 eV) to model the injection dependent minority carrier lifetime measurements from selected n- and p-type samples. One important point to retain from our previous discussion is that the capture cross-section ratio $k = s_n / s_p \sim 1$ for the defect responsible for lifetime degradation in samples that have received RIE. The benefits of knowing this fact are twofold. Firstly, it relieves us of the problem that DLTS provides a measure of only the majority carrier capture cross-section of a defect. Secondly, for any given sample resistivity, we only have to show simulations for either an n-type or a p-type sample (Fig. 3). For completeness, we have included Auger recombination, which impacts at high excess carrier densities, in the modelling procedure [10]. Our methodology also allows the effect of minority carrier trapping, which may become pronounced in the low carrier injection regime, to be simulated [11]. The latter phenomenon may give rise to an apparent increase in effective lifetime in low-injection due to the temporary trapping of minority carriers followed by their subsequent release.

The solid lines in Figure 5 demonstrate that the experimental data points (open symbols) can be adequately simulated following the SRH formalism and using the "signature" of B(0.32 eV). However, this observation has to be qualified. Firstly, there are large uncertainties associated with the capture cross-section used in this study. Consequently, the defect concentrations used in simulations do not necessarily correlate with those estimated from DLTS measurements [1]. Further, it is pointed out that many other combinations of E_t and s_a may also provide reasonable fits to the experimental data, since the equation describing the SRH formalism contains too many free paramters. Nevertheless, the simulations in Fig. 5 at least show that an energy level of 0.32eV is not *inconsistent* with the measured injection dependence of minority carrier lifetime in samples that received RIE. Note that the injection dependence of the lifetime is quite flat, consistent with the defect having approximately equal capture cross sections, and hence a similar impact in both n- and p-type silicon.

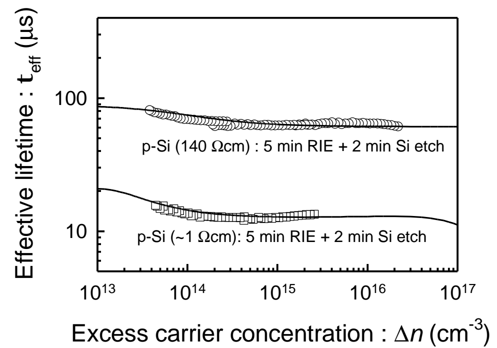

Figure 5: Modelling the injection dependent minority carrier lifetime of reactive ion etched p-Si samples

6 SUMMARY

In summary, we have used the combination of QSSPC and DLTS to characterize the minority carrier lifetime properties of reactive ion etched FZ p-Si. RIE proceeds by the simultaneous build up of damage in the near-surface region of the exposed Si and etching of the damaged layer by physical-chemical etching. The initial stage of RIE is dominated by the first process. Thereafter,

a steady-state is reached when the two competing processes equilibrate. Our results have confirmed the long-range migration (exceeding 2 μm) of defects generated by RIE at room temperature. We have also shown that the lifetime degradation by RIE was independent of the type of substrate used, revealing that the defect level(s) acting as a recombination centre(s) had similar capture cross sections for holes and electrons, and that the defect did not involve dopant species. The electronic properties of a hole trap B(0.32 eV) were used to adequately model the injection dependent minority carrier lifetime in the plasma-etched samples. Our results have shown that QSPCC and DLTS form a powerful combination of analytical techniques for the characterization of defects that are relevant for the performance of solar cells.

7 ACKNOWLEDGEMENT

The authors would like to acknowledge the financial support of the Australian Research Council.

8 REFERENCES

[1] P.N.K. Deenapanray, M. Hoertis, D. Macdonald, K.J. Weber, Electrochem. Solid-State Lett. 8 (2005) G78, and references therein.
[2] S. Schaefer, R. Ludeman, J. Vac. Sci. Technol. A 17 (1999) 749.
[3] V. Gazuz, K. Feldrapp, R. Auer, R. Brendel, M Schulz, Solar Energy Mat. & Solar Cells 72 (2002) 277.
[4] K.J. Weber, A.W. Blakers, M.J. Stocks, J.H. Babaei, V.A. Everett, A.J. Neuendorf, P.J. Verlinden, IEEE Electron Dev. Lett. 25 (2004) 37.
[5] R.A. Sinton, A. Cuevas A, Appl. Phys. Lett. 69 (1996) 2510.
[6] S. Rein, T. Rehrl, W. Warta, S.W. Glunz, J. Appl. Phys. 91 (2002) 2059.
[7] P.N.K. Deenapanray, C. Nyamhere, F.D. Auret, Paper presented at this conference.
[8] P.M. Mooney, L.J. Cheng, M. Süli, J.D. Gerson, J.W. Corbett, Phys. Rev. B8 (1977) 3836.
[9] A. Khan, M. Yamaguchi, Y. Ohshita, N. Dharmarasu, K. Araki, T. Abe, H. Itoh, T. Ohshima, M. Imaizumi, S. Matsuda, J. Appl. Phys. 90 (2001) 1170.
[10] M.J. Kerr, A. Cuevas, J. Appl. Phys. 91 (2002) 2473.
[11] D. Macdonald, A. Cuevas, Appl. Phys. Lett. 74 (1999) 1710.